frontiers | Frontiers in Earth Science

ORIGINAL RESEARCH
published: 15 July 2022
doi: 10.3389/feart.2022.846245

Marine Paleoproductivity From the Last Glacial Maximum to the Holocene in the Southwestern Atlantic: A Coccolithophore Assemblage and Geochemical Proxy Perspective

Guilherme A. Pedrão[1], Marcus V. Hirama[1], Mariana O. Tomazella[1], Ana Luiza S. Albuquerque[2], Cristiano M. Chiessi[3], Karen B. Costa[1] and Felipe A. L. Toledo[1]*

[1]Instituto Oceanográfico, Universidade de São Paulo, São Paulo, Brazil, [2]Programa de Geociências (Geoquímica), Universidade Federal Fluminense, Niterói, Brazil, [3]Escola de Artes e Ciências Humanas, Universidade de São Paulo, São Paulo, Brazil

OPEN ACCESS

Edited by:
Michaël Hermoso, UMR8187 Laboratoire d'océanologie et de géosciences (LOG), France

Reviewed by:
Hongrui Zhang, ETH Zürich, Switzerland
Xinquan Zhou, Tongji University, China

***Correspondence:**
Guilherme A. Pedrão
guilherme.pedrao@usp.br

Specialty section:
This article was submitted to Quaternary Science, Geomorphology and Paleoenvironment, a section of the journal Frontiers in Earth Science

Received: *30 December 2021*
Accepted: *13 June 2022*
Published: *15 July 2022*

Citation:
Pedrão GA, Hirama MV, Tomazella MO, Albuquerque ALS, Chiessi CM, Costa KB and Toledo FAL (2022) Marine Paleoproductivity From the Last Glacial Maximum to the Holocene in the Southwestern Atlantic: A Coccolithophore Assemblage and Geochemical Proxy Perspective. Front. Earth Sci. 10:846245. doi: 10.3389/feart.2022.846245

In this study, we associated the variations in coccolithophore assemblages with the variability in major elements (Fe, Ca, and Ti) from the continental slope of the western South Atlantic by investigating two marine sediment cores (GL-824 and GL-1109) to reconstruct paleoceanographic and paleoproductivity changes from the Last Glacial Maximum (LGM) to the present. Terrigenous-supply proxies (Fe/Ca and Ti/Ca) showed a very similar pattern compared with the fine-fraction sediments, higher values throughout the LGM and lower values during the Holocene. The dominant species in the coccolithophore assemblages were *Emiliania huxleyi*, *Gephyrocapsa* spp., and *Florisphaera profunda*, with these species together representing between 82 and 99% of the total assemblage. Additionally, we used three other subordinate species (*Umbellosphaera* ssp., *Rhabdosphaera* spp., and *Syracosphaera* spp.) for paleoproductivity reconstruction. The estimates of primary production using *F. profunda* and *Gephyrocapsa* spp. exhibited a similar trend, with higher productivity values during the LGM. Paleoproductivity decreased toward the Late Holocene. Analyzing these results, we observed that the oscillation of relative sea level was the process that controlled paleoproductivity, primarily by changing the position of the main flow of the Brazil Current (BC). During periods of high sea level (low Fe/Ca and Ti/Ca), the BC transported warm and oligotrophic water to the upper slope, preventing any nutrient transport from deeper layers or coastal water. In contrast, during low sea-level periods (high Fe/Ca and Ti/Ca), the offshore displacement of the BC allowed the presence of coastal water (more nutrient-rich than tropical water) and the erosion of the exposed shelf that along with a more enhanced fluvial input provided more nutrients to the photic zone, thus enhancing primary productivity.

Keywords: paleoproductivity, X-ray fluorescence, Fe/Ca, Ti/Ca, Brazil Current

1 INTRODUCTION

Studying the variations in oceanic parameters over time is extremely important to understand their influence on climate because the ocean is one of the largest carbon reservoirs on the planet. In addition, marine phytoplankton uses carbon dioxide and ocean surface sunlight to generate organic matter through photosynthesis. Therefore, oceanic productivity plays a unique role in this system because changes in the strength of the biological pump might be one of the processes controlling the CO_2 variations in glacial/interglacial time scales. In this context, the Last Glacial Maximum (LGM) is a significant contrasting period compared with the actual warming trend. During the LGM, the CO_2 concentration was about 50% lower than the present values, atmospheric temperatures were cooler, and the ice sheets cover was at its maximum, leaving the sea level at its minimum. Thus, studying this steady state of the glacial word is essential, even for assisting model studies in boundary conditions.

Marine sediments record climate and oceanographic variations by means of chemical element variations during a specific period. In this study, we employ the relative concentrations of chemical elements, titanium (Ti), iron (Fe), and calcium (Ca), to infer terrigenous sediment contributions. Ca mainly reflects marine carbonate content; Ti and Fe, on the other hand, are related to siliciclastic content (Arz et al., 1998; Jansen et al., 1998; Govin et al., 2012a). Therefore, the variations in these elements allow us to obtain paleoclimatic and paleoceanographic information about the study area. Several authors have applied Fe/Ca and Ti/Ca ratios to trace-element changes in terrigenous input of mainly fluvial origin, particularly offshore northeastern Brazil (Arz et al., 1998; Arz et al., 1999; Jaeschke et al., 2007).

The Brazilian margin is an important region to study climate changes because the Brazil Current directly influences it. This western boundary current transports warm oligotrophic water from the tropics to subtropics, affecting the local environment and productivity. Thus, marine paleoproductivity reconstructions associating changes in these processes, especially in the continental slope and shelf transition, are crucial to understanding the interplay between the continental and marine environments.

Paleoproductivity along the southeastern Brazilian upper slope has been correlated with hydrodynamic changes driven by sea-level fluctuations that during glacial periods would promote the offshore displacement of the Brazil Current leading to higher marine productivity in the continental shelf and upper slope (Mahiques et al., 2007; Nagai et al., 2010; Nagai et al., 2014; Lourenço et al., 2016; Pereira et al., 2018). Previous paleoproductivity studies for the region were based on the variation in foraminiferal assemblages (Nagai et al., 2010; Pereira et al., 2018), the evaluation of sedimentary changes (Mahiques et al., 2007), and the use of organic biomarkers (Lourenço et al., 2016). A multiproxy approach combining all these indicators is a more reliable perspective since any given proxy has limitations. For instance, the benthic foraminiferal accumulation rate (Nagai et al., 2010) and total organic carbon accumulation might be influenced by changes in preservation and sedimentation rates (Rühlemann et al., 1999; Lourenço et al., 2016). Benthic (Nagai et al., 2010) and planktonic foraminiferal assemblage analyses (Pereira et al., 2018) are excellent paleoproductivity proxies. However, they provide an indirect paleoproductivity perspective because planktonic foraminifera are mainly heterotrophic, feeding on smaller organisms, organic matter, and phytodetritus. Furthermore, coccolithophores offer us a unique and more direct vision of productivity.

Coccolithophores are unicellular microalgae belonging to the Haptophyte division and they have an inorganic envelope of calcium carbonate ($CaCO_3$) composed mainly of calcite, known as the coccosphere, formed by a series of small plates called coccoliths. Coccolithophores are among the most significant components of calcium carbonate in seafloor sediments and they are the major carbonate-shelled primary producer group with extensive geographic fossil preservation during the Quaternary (Stoll and Ziveri, 2002). As primary producers, environmental parameters control coccolithophore distribution and include nutrient availability, light, and temperature (Winter et al., 1994). These factors make this fossil group a valuable tool in paleoceanographic and paleoproductivity reconstructions (Flores et al., 1999, 2000; Toledo et al., 2007; Saavedra-Pellitero et al., 2011; Leonhardt et al., 2013; Cabarcos et al., 2014; Costa et al., 2016). Therefore, combining coccolithophore records with geochemical sedimentary proxies is ideal for understanding how climate change in past environments affected these organisms, especially in regard to paleoproductivity (Zhou et al., 2020).

The main goal of this study is to acquire information about the paleoproductivity record based on coccolithophore assemblage variations and the contribution of terrigenous supply in the marine sedimentary record. Then, we analyzed the observed variations to infer paleoenvironmental changes connected to processes that could modify the paleoclimate and paleoceanography of southeastern Brazil.

2 REGIONAL SETTING

The Brazil Current (BC) dominates surface circulation in this region (**Figure 1**). This current originates from the southern branch of the South Equatorial Current (SEC) bifurcation around 10° S latitude. The BC flows southward, carrying mainly warm and saline water flowing along the shelf-break isobaths, with possible meandering occurring close to the shelf. This current is usually 100 km wide, with its extension flowing in the upper 500 m (Silveira et al., 2000). The BC has a so-called "floor polisher effect" that regularly does not allow the deposition of thinner sediments, leading to a marine bottom composed mainly of coarse sand and carbonate gravel (Mahiques et al., 2002).

The major water masses that compose the upper water column are Coastal Water (CW), Tropical Water (TW), and South Atlantic Central Water (SACW). CW is located on the continental shelf, containing a mix of oceanic water with water from continental drainage (Campos et al., 1999). In offshore regions, the BC transports, at the surface, warm and saline water of the TW and, at the pycnocline, the colder and

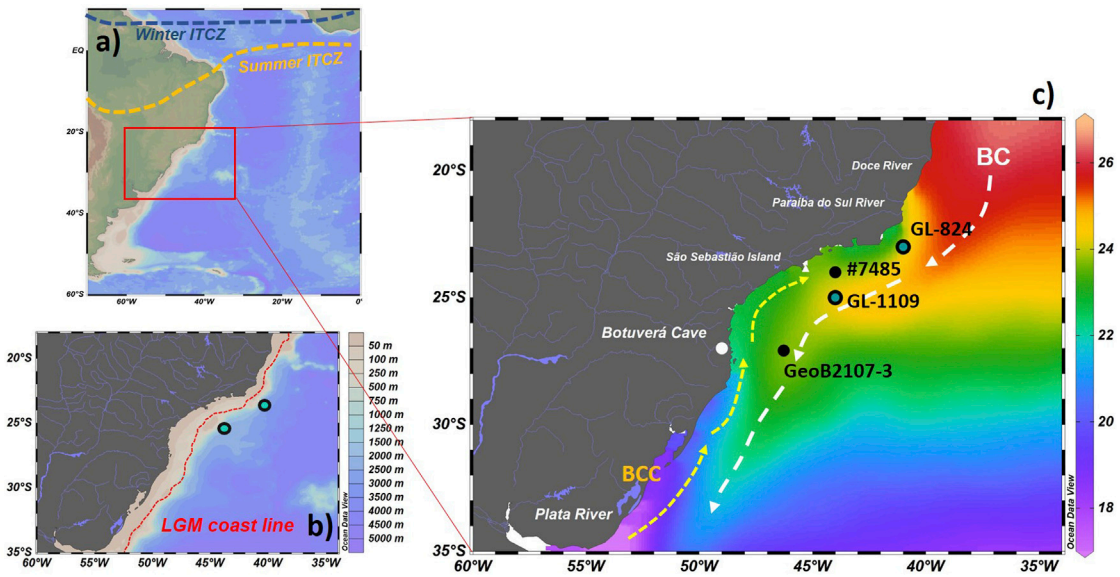

FIGURE 1 | (A) Location of the southwestern Atlantic margin. The dashed lines represent the position of the ITCZ during winter (blue) and summer (yellow). **(B)** Magnified view of the bathymetry of the study area with the approximate coastline during the LGM. **(C)** The annual mean sea surface temperature is represented °C (Locarnini et al., 2018). Blue dots mark the cores used in the present study (GL-824 and GL-1109). Cores #7485 (Lourenço et al., 2016) and GeoB2107-3 (Pereira et al., 2018) with data shown in the discussion are represented by black dots. The white dots represent the central geographic locations cited in this work. The dashed white arrows represent the main flow of the Brazil Current, while the yellow arrows show the main flow of the Brazilian Coastal Current.

nutrient-rich SACW (Silveira et al., 2000). In the deeper portions of the water column, there are movements of two relevant deep water masses: the Deep Western Boundary Current transports the North Atlantic Deep Water (NADW), which flows southward, and the Antarctic Bottom Water (AABW), which flows northward as a sluggish flow above the ocean floor (Stramma and England, 1999; Silveira et al., 2020). According to Vianna et al. (1998), changes in relative sea level (RSL) are the primary cause of oceanic circulation variations during the Quaternary.

The main controlling forces of modern sedimentary processes on the southeastern Brazilian margin are the BC system flow variations and the dynamics between the continental shelf and oceanic water masses (Mahiques et al., 2004). There is a division in sedimentation on the continental shelf into two distinct zones separated by São Sebastião Island. In the north, meandering of the BC, which promotes mixing between terrigenous and pelagic sedimentary fractions, is the primary control of sedimentation. On the other hand, the southern sector is characterized mainly by marine sedimentation. Infiltration of the Plata River plume directly influences this region because there is a lack of a local fluvial supply (Mahiques et al., 2004). This process transports more terrigenous sediments and nutrients to the surface water, increasing oceanic productivity (Ciotti et al., 1995; Pivel et al., 2011; Nagai et al., 2014; Bícego et al., 2021). The fluvial supply is a vital sediment source in the northern section of the study area. The main rivers that conduct terrigenous sediments in this area are the Doce River and Paraíba do Sul River (Behling et al., 2002). At glacial and interglacial scales, sea level variations and climate conditions on the adjacent continent, particularly precipitation, are factors that may influence the terrigenous sediment supply to the continental slope (Mahiques et al., 2004; Nagai et al., 2014; Razik et al., 2015; Zhou et al., 2020).

The southwestern Atlantic is an oligotrophic zone (Rühlemann et al., 1999) where nutrient concentration is the key factor limiting primary productivity. Local fluvial discharge (Brandini et al., 2014) and upwelling associated with cyclonic meanders of the BC occur throughout the entire year (Campos et al., 1995; Campos et al., 2000), increasing photic-zone nutrient concentration. In a seasonal pattern, wind-driven coastal upwelling peaks during austral summer and enhances shelf-break upwelling that occurs due to the meanders of the BC, causing higher rates of primary productivity (Campos et al., 2000; Brandini et al., 2014). During winter, the Plata River plume transports more nutrients to the study area under favorable wind conditions (Campos et al., 1999; Piola et al., 2005; Pivel et al., 2011). Therefore, the interplay between the dynamics of the BC and the continental source nutrients characterizes the primary productivity of the region.

The South American Summer Monsoon (SASM) controls precipitation in the study region (Vera et al., 2006), which varies according to its intensity and expansion. Therefore, precipitation has a strong seasonal pattern, with most precipitation occurring during summer. In this period, SASM circulation transports moisture from the Atlantic Ocean to the Amazon Basin, feeding the low-level jets of the Andes and transporting this moisture to southeastern Brazil (Cheng et al., 2013), entering the South Atlantic Convergence Zone (SACZ). Throughout Quaternary glacial–interglacial climate change, during glacial periods, in contrast to interglacial periods, there was a reinforcement of the SASM, especially during the Last Glacial Maximum (LGM), transporting more humidity to

TABLE 1 | Radiocarbon ages based on planktonic foraminifera from the GL-824 core. Both white (w) and pink (p) *G. ruber* morphotypes were used.

Depth (cm)	Foraminifera species	Age ^{14}C (years BP)
0	*G. ruber*	200 ± 50
205	*G. ruber*	1960 ± 30
400	*G. ruber*	3,750 ± 35
620	*G. ruber*	6,080 ± 45
820	*G. ruber*	8,140 ± 50
947	*G. ruber*	9,780 ± 60
1,020	*G. ruber*	10,400 ± 60
1,220	*G. ruber*	13,050 ± 85
1,420	*G. ruber* and *G. sacculifer*	13,100 ± 70
1,620	*G. ruber* and *G. sacculifer*	15,650 ± 110

southern Brazil (Sylvestre, 2009). The SACZ is a zone oriented in a northwest-southeast direction characterized by converging winds, considerable cloud cover, and heavy precipitation (Liebmann et al., 2004; Carvalho et al., 2002, 2004), with most extreme events of precipitation over southeastern Brazil occurring during summer being associated with intensification of the SACZ (Carvalho et al., 2002).

The position of the Intertropical Convergence Zone (ITCZ) directly influences the intensity of the SACZ and is the zone near the equator where the northeast and southeast trade winds converge, forming a band of clouds. The position of the ITCZ has a seasonal variation. It migrates toward the hemisphere that is warmer relative to the other (Deplazes et al., 2013; Schneider et al., 2014). During austral summer, the ITCZ is in its southernmost position, and in winter, it migrates to its northerly position (**Figure 1**).

3 MATERIALS AND METHODS

3.1 Sediment Core Recovery

Two marine sediment cores, GL-824 and GL-1109, were collected on the Brazilian continental margin; more precisely, on the continental slope, GL-824 core was collected at a water depth of 532 m at 23°29′17,87″ S and 41°08′02,99″ W, while GL-1109 was located at a water depth of 848 m at 25°11′00″ S and 44°43′30″ W (**Figure 1**). Sediment core GL-824 was collected during an expedition with the Fugro Explorer Vessel. A piston corer was used to recover 2004 cm of sediment. This work analyzes 100 samples at an average 20 cm resolution. According to the lithology, the first 1,500 cm is composed of olive-gray carbonate-rich mud (18–30% $CaCO_3$), and from 1,550 to 2004 cm, the sediment is composed of dark gray carbonate-poor mud (5–18% $CaCO_3$). GL-1109 had a total recovery of 1,367 cm of marine sediment. This work analyzes the section from 515 cm to the top of the core, sampling approximately every 5 cm, with 95 samples investigated. According to the lithology, the core comprises dark gray carbonate-poor mud (5–18% $CaCO_3$).

3.2 Age Model

The age model of both cores was constructed based on radiocarbon dating conducted mainly on the planktonic foraminifer *Globigerinoides ruber* (white and pink morphotypes). In the absence of *G. ruber*, we collected other species, such as *Globigerinoides sacculifer* (>150 μm size) and *Globigerina bulloides* (**Table 1**), with all of these species exhibiting a good preservation state and no overgrowth or dissolution effects. For the GL-824 core, 11 samples were selected and analyzed at the National Ocean Science Accelerator Mass Spectrometer Facility (NOSAMS), Woods Hole Oceanographic Institution (WHOI) (**Table 1**). For GL-1109, 19 samples were analyzed at the Beta Analytic Radiocarbon Dating Laboratory, Miami, United States (**Table 2**).

To transform the radiocarbon ages into calibrated ages, we used the calibration curve Marine13 (Reimer et al., 2013) and a marine reservoir age of 370 ± 19 years (Alves et al., 2015) with Bacon 2.2 software (Blaauw and Christen, 2011). This software constructs the age model using Bayesian statistics and estimates mean ages and 95% error margins based on 10,000 downcore age-depth realizations at a 1 cm resolution. To establish the ages, we applied the default parameters, except for the calibration curve, in which we selected Marine13 and acc. shape (set to 0.5).

3.3 Sample Preparation and Fine Fraction Quantification

The bulk samples were wet sieved through a 63 μm mesh. The coarse fraction (>63 μm) was dried on the mesh in an oven at 50°C and allowed to cool before weighing. The fine fraction (<63 μm) was collected in beakers where it was allowed to settle. The water was removed, and the samples were dried in an oven at 50°C and allowed to cool before weighing. To calculate the fine fraction (FF) percentage in every sample, we used the difference in weight between the coarse fraction and the total dried weight of the sample. The FF was used for all the procedures and analysis described below, except for GL-1109 elementary composition measurements.

3.4 Calcium Carbonate

The carbonate content was measured by the difference in weight before and after acidification with HCl. Approximately 1.0 g of dry sediment was weighed and acidified with 10% HCl. The sample was kept overnight, and the supernatant was discarded. Then, distilled water was added (3 times) to the sample for acid removal. Finally, the precipitated sample was kept at 60°C in an oven overnight and weighed again. The difference in weight before (Weight 1) and after reaction with HCl (Weight 2) provides an approximate estimate of the carbonate content %: $CaCO_3$ = [(Weight 1 − Weight 2) × 100)/Weight 1].

3.5 X-Ray Fluorescence

The samples were powdered and homogenized with an agate mortar to calculate the elementary ratios in GL-824 core. Then, metals (Ti, Fe, and Ca) were analyzed in a bench equipment model BTX-II to perform X-ray fluorescence measurements in the Laboratory of Geoprocessing (LabGEO-USP), following the technique described in Pedrão et al. (2021). Briefly, the technique consists of analyzing the metals in approximately 1 cm^3 of sediment (<63 μm) per sample that was previously hand-

TABLE 2 | Radiocarbon ages based on planktonic foraminifera from the GL-1109 core. Both white (w) and pink (p) *G. ruber* morphotypes were used.

Depth (cm)	Foraminifera species	Age ^{14}C (years BP)	
1	*G. ruber* (w)	120 ± 30	
17	*G. ruber* (w)	970 ± 30	
31	*G. ruber* (w)	2,360 ± 30	
53	*G. ruber* (w)	3,980 ± 30	
75	*G. ruber* (w)	6,200 ± 30	
101	*G. ruber* (w)	8,790 ± 30	
143	*G. ruber* (w+p), *G. sacculifer*, and *G. bulloides*	12,840 ± 50	
291	*G. ruber* (w+p), *G. sacculifer*, and *G. bulloides*	16,170 ± 60	
331	*G. ruber* (w+p), *G. sacculifer*, and *G. bulloides*	16,310 ± 60	
365	*G. ruber* (w+p)	16,690 ± 50	
463	*G. ruber* (w+p), *G. sacculifer*, and *G. bulloides*	17,810 ± 80	
507	*G. ruber* (w+p), *G. sacculifer*, and *G. bulloides*	19,420 ± 70	Age reversal
563	*G. ruber* (w+p), *G. sacculifer*, and *G. bulloides*	18,820 ± 60	
597	*G. ruber* (w+p), *G. sacculifer*, and *G. bulloides*	20,470 ± 80	
663	*G. ruber* (w+p), *G. sacculifer*, and *G. bulloides*	22,350 ± 80	
793	*G. ruber* (w)	28,300 ± 140	
825	*G. ruber* (w)	28,970 ± 150	
857	*G. ruber* (w)	31,280 ± 190	
938	*G. ruber* (w)	36,950 ± 330	
967	*G. ruber* (w)	40,730 ± 500	

ground in a jade mortar to be used in the XRF analysis. We selected this size fraction due to the more negligible interference in the intensity values measured by the device. In GL-1109 core, we analyzed the elementary composition of the sediments by conducting an XRF analysis using an XRF Core–Scanner II (AVAATECH Serial No. 2) at MARUM, University of Bremen, to estimate the elementary ratios throughout the core.

The geochemical data were presented in the logarithmic form of elemental ratios since ratios are insensitive to dilution effects (Wetje and Tjallingii, 2008; Govin et al., 2012b), and the logarithmic form accounts for the lack of symmetry between ratios (Govin et al., 2012b).

3.6 Coccolithophore Assemblages

The qualitative technique described by Antunes (1997) and Toledo (2000) was utilized to prepare samples to identify and quantify the coccolithophore assemblages in terms of percentages. Counts were made under a polarized light microscope at a 1,000X magnification. A minimum of 300 coccoliths, in addition to *Florisphaera profunda* coccoliths, were counted in each sample, assuring that all species with relative abundances greater than 3% were well represented (Dennison and Hay, 1967; Roth, 1994; Fatela and Taborda, 2002). *Florisphaera profunda* was excluded from the 300 coccoliths minimum counts because it may dominate the assemblages and mask the signal of other species. However, the total number of coccolithophore species, including *F. profunda*, was used for calculating the relative abundances of coccoliths.

Variations between the relative abundance of the main species in the upper photic zone (*Emiliania huxleyi* and *Gephyrocapsa* spp.) and the lower photic zone (*F. profunda*) can be used as indicators of primary productivity (e.g., Beaufort et al., 1997, 2001; Flores et al., 2000). *Florisphaera profunda* is an habitant in the lower photic zone (LPZ) (Okada and Honjo, 1973) and is commonly used as a paleoproductivity proxy (Beaufort et al., 2001; Hernandez-Almeida et al., 2019), mainly because this species is an indicator of the thermocline/nutricline position (Molfino and McIntyre, 1990; Flores et al., 2000). When more nutrients are available in the upper photic zone (UPZ), opportunistic species such as *Gephyrocapsa* spp. and *E. huxleyi* increase in abundance, while *F. profunda* decreases in relative abundance. In contrast, when the nutricline is greater, more nutrients are available for species in the LPZ, such as *F. profunda*, raising their relative abundance compared to the UPZ dwellers. Therefore, Beaufort et al. (1997) established an equation to estimate primary productivity (EPP, grams of carbon ((gC) m^{-2} $year^{-1}$)) based on the relative abundance of *F. profunda* (Fp, %) [EPP = 617 − (279 log(Fp + 3))].

To evaluate the effect of dissolution in our record, we applied the CEX' index (Boeckel and Baumann, 2004), which compares the relative abundances of the small and more sensitive species, *Gephyrocapsa* spp. and *E. huxleyi*, to the more resistant large species, such as *Calcidiscus leptoporus*. The index varies between 1 and 0, with values close to 1 indicating no dissolution and values below 0.6 indicating a more substantial dissolution influence.

We applied the Pearson linear correlation index (r) using Past 3.05 software (Hammer et al., 2001) in both cores separately to investigate the associations among sedimentology and geochemical and micropaleontological proxies.

4 RESULTS

4.1 Age Model

The results of 11 radiocarbon ages for GL-824 show continuous sedimentation (**Figure 2A**), which indicates that no hiatus occurred in the core. The core covers an age range of approximately 22 kyrs BP with an average accumulation rate of approximately 97 cm/kyrs (**Figure 2A**), with the lowest sedimentation rate occurring in the Early Holocene (~70 cm/

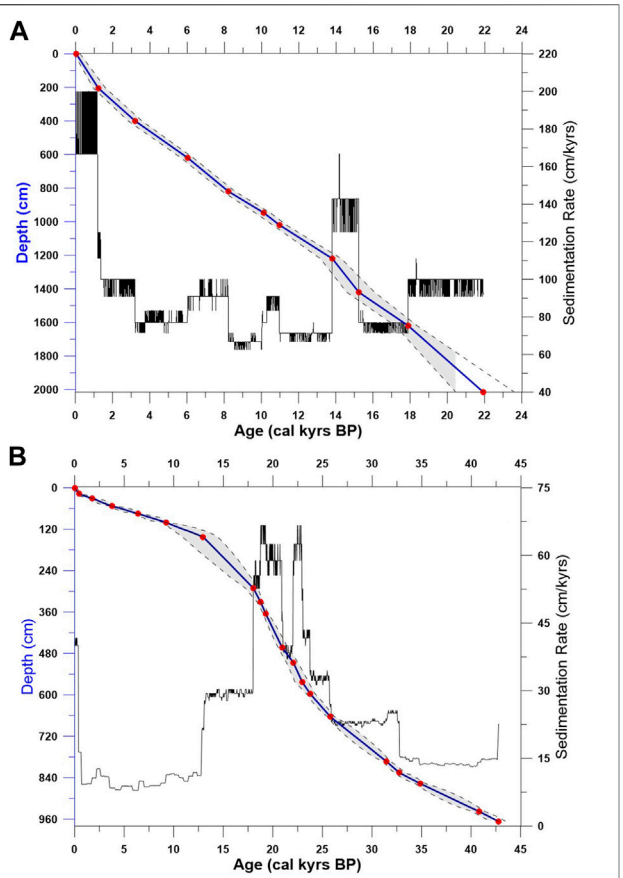

FIGURE 2 | Age model (solid line) and sedimentation rates for the **(A)** GL-824 and **(B)** GL-1109 cores. The red dots represent the calibrated radiocarbon ages, while the dashed lines are the upper and lower confidence intervals. We applied Bacon 2.2 software (Blaauw and Christen, 2011) to build this age model.

kyrs) and the highest occurring at its top (~180 cm/kyrs) and between 14 and 15 kyrs BP (~150 cm/kyrs).

Even though we observed an age reversion in GL-1109 core (**Table 2**), using Bacon 2.2, we constructed an age model that represents continuous sedimentation with no hiatus (**Figure 2B**). The core comprises the last 45 kyrs BP. However, this study only analyzed the top 550 cm of the core at a resolution of 2–5 cm between samples, comprising the last 23 kyrs BP. This section had a medium sedimentation rate of 38 cm/kyrs, with significant sedimentation occurring in the LGM period between 25 kyrs BP and 19 kyrs BP (65 cm/kyrs). The sedimentation rate then decreased until 12 kyrs BP, reaching the lowest value, 8 cm/kyrs (**Figure 2B**).

4.2 Sedimentary Record

The proxies for terrigenous sediment supply in both cores show a similar distribution to the FF content (**Figures 3A–F**). Higher values of terrigenous supply and FF percentage were recorded at the bottom of the cores during the glacial period, with almost all samples having 100% FF and top metal content. In Core GL-824, a marked decrease was recorded at approximately 15 kyrs BP,

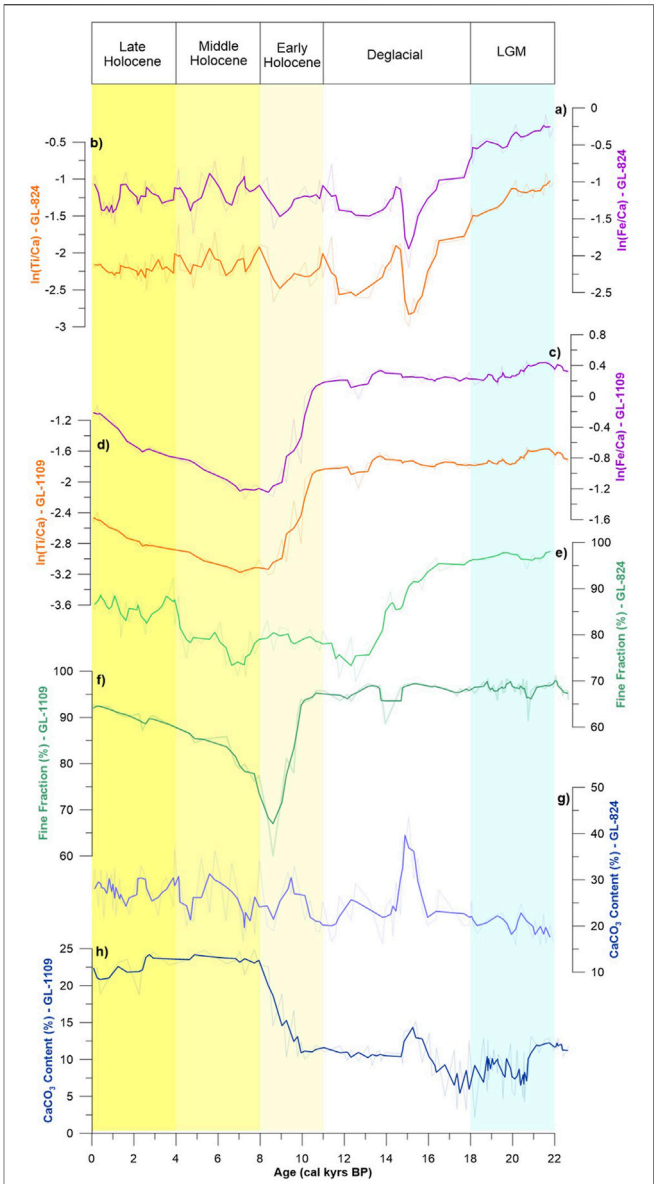

FIGURE 3 | Results of the sedimentary record from GL-824 and GL-1109 cores. Thick lines represent a weighted average of 3 points, and the background lines are the original data. **(A)** ln (Fe/Ca) and **(B)** ln (Ti/Ca) results for GL-824. **(C)** ln (Fe/Ca) and **(D)** ln (Ti/Ca) results for GL-1109. **(E)** Percentage of fine fraction present in the GL-824 core. **(F)** Percentage of fine fraction present in the GL-1109 core. **(G)** Calcium carbonate content throughout the GL-824 core. **(H)** Calcium carbonate content throughout the GL-1109 core.

with the proxies reaching their minimum values. However, in GL-1109 core, it occurred at the beginning of the Holocene (~11 kyrs BP).

The $CaCO_3$ content was the most divergent parameter between the cores, with higher mean values in GL-824 (25%) than in GL-1109 (13%). The $CaCO_3$ content presented the same general trend between the cores, with lower values in the late glacial period and a rapid rise during the transition between the deglacial period and the early Holocene (16–8 kyrs BP), reaching

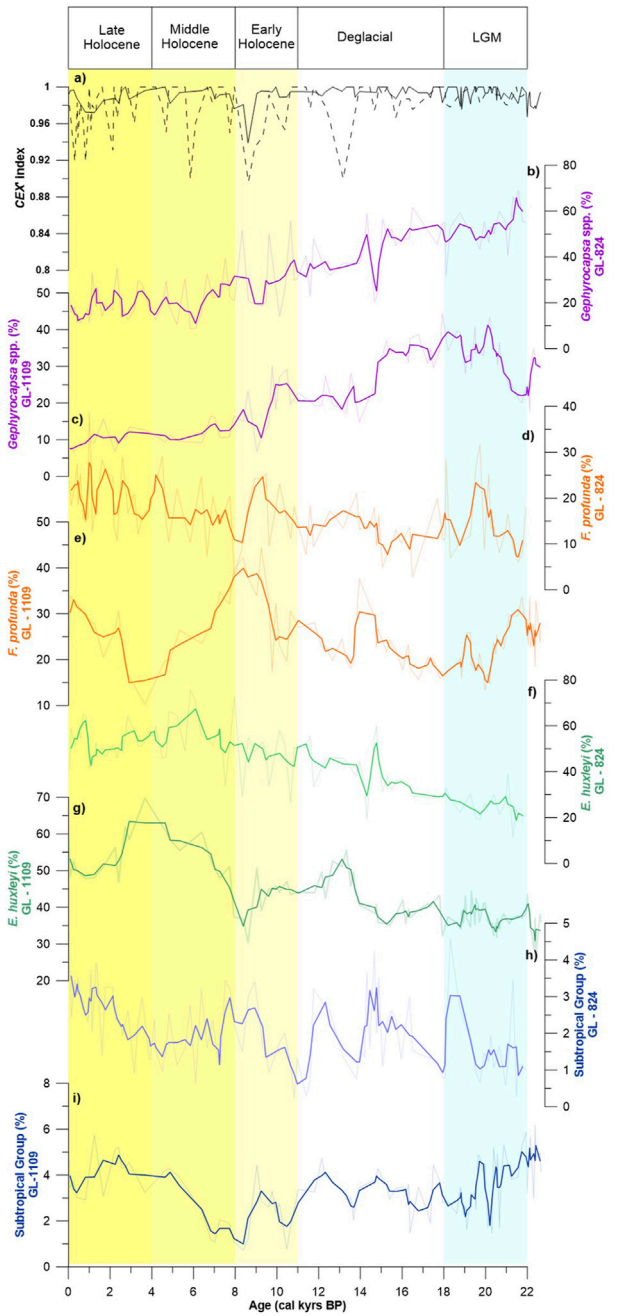

FIGURE 4 | Results of the coccolithophore assemblages from GL-824 and GL-1109 cores. Thick lines represent a weighted average of 3 points, and the background lines are the original data. **(A)** CEX′ index for both cores. The solid line represents GL-824 core, and the dashed line represents GL-1109 core. **(B)** Relative abundance of *Gephyrocapsa* spp. in the GL-824 core. **(C)** Relative abundance of *Gephyrocapsa* spp. in the GL-1109 core. **(D)** Relative abundance of *F. profunda* in the GL-824 core. **(E)** Relative abundance of *F. profunda* in the GL-1109 core. **(F)** Relative abundance of *E. huxleyi* in the GL-824 core. **(G)** Relative abundance of *E. huxleyi* in the GL-1109 core. **(H)** Relative abundance of the subtropical group in the GL-824 core. **(I)** Relative abundance of the subtropical group in the GL-1109 core.

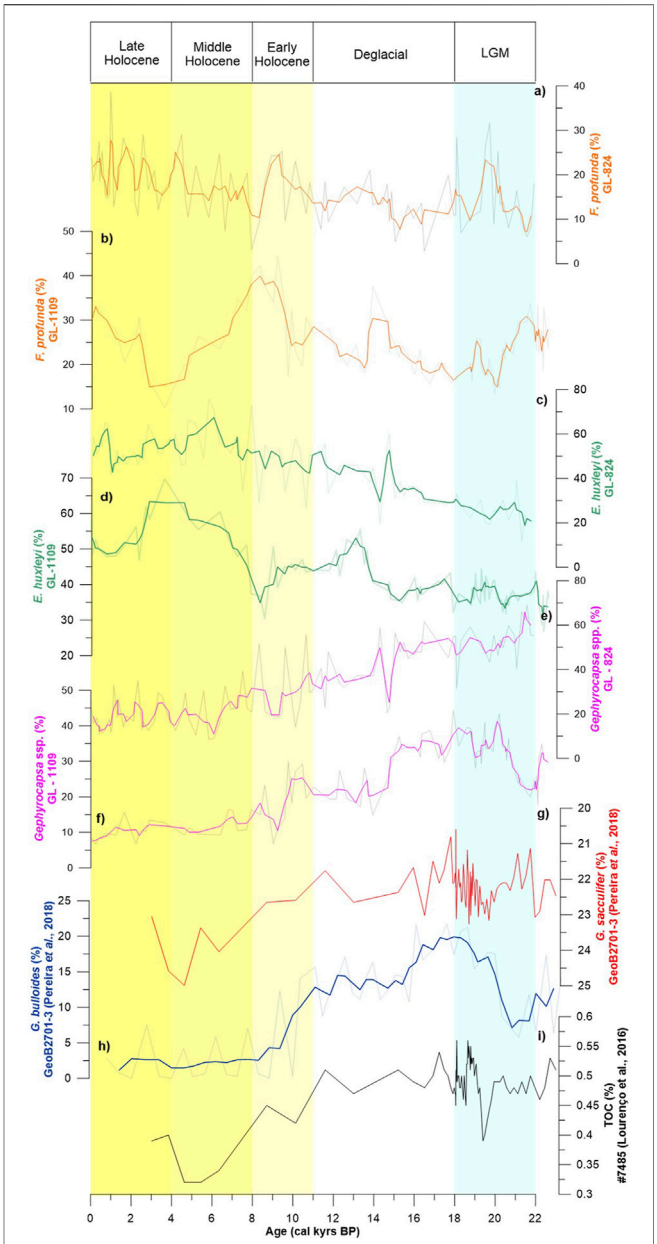

FIGURE 5 | Paleoproductivity proxy results. Thick lines represent a weighted average of 3 points, and the background lines are the original data. **(A)** *F. profunda* relative abundance for the GL-824 core. **(B)** *F. profunda* relative abundance for the GL-1109 core. **(C)** Relative abundance of *E. huxleyi* in the GL-824 core. **(D)** Relative abundance of *E. huxleyi* in the GL-1109 core. **(E)** *Gephyrocapsa* spp. relative abundance for the GL-824 core. **(F)** *Gephyrocapsa* spp. relative abundance for the GL-1109 core. **(G)** Relative abundance of the oligotrophic planktonic foraminifera *G. sacculifer* (Pereira et al., 2018). **(H)** Relative abundance of *G. bulloides*, an upwelling proxy (Pereira et al., 2018). **(I)** TOC content (Lourenço et al., 2016).

higher values toward the mid-Holocene (**Figures 3G,H**). This trend was opposite to the distribution observed in the elementary ratios and FF (**Figures 3E–H**).

4.3 Coccolithophore Assemblages

Coccolithophore assemblage variations (**Figure 4**) had the same general variations in both cores. The dominant species were *E. huxley*, *Gephyrocapsa* spp., and *F. profunda*, representing 82–99% of the total assemblage in GL-824 and 85–97% in GL-1109. The mean relative abundances for the dominant species were 43–42% for *E. huxleyi*, 33–25% for *Gephyrocapsa* spp., and 16–24% for *F. profunda* (first valor for GL-824 and second for GL-1109). *Gephyrocapsa oceanica* (mean relative abundance = 15%) was the most common species in *Gephyrocapsa* (**Figures 4B,C**). The CEX' index had high values in the entire core (**Figure 4A**), indicating that dissolution was not a problem in regard to paleoenvironmental interpretations. The relative abundances of *F. profunda* and *E. huxleyi* had a similar trend. The lowest values occurred during the glacial period, with a gradual increase toward the deglacial period, reaching higher values during the Holocene (**Figures 4D–G**). In contrast, *Gephyrocapsa* spp. had an opposite distribution, with higher values during the glacial period and lower values in the Holocene (**Figures 4B,C**).

Discosphaera tubifera, *Rhabdosphaera* spp., *Syracosphaera* spp., and *Umbellosphaera* spp. composed a subtropical group with a tendency toward warmer and oligotrophic water conditions, as suggested by Boeckel et al. (2006). The relative abundance of this group showed a similar trend as that of *F. profunda* (**Figures 4H, 1**). However, low relative abundances appeared, with a mean value of 2% in GL-824 and 3.5% in GL-1109.

The N ratio proposed by Flores et al. (2000) compares the relative abundances of LPZ species (*F. profunda*) with those of the UPZ (*Gephyrocapsa* spp. and *E. huxleyi*); thus, this ratio can be used as an indicator of the nutricline position and, therefore, of primary productivity. The N ratio and EPP presented a similar general pattern in the cores (**Supplementary Figure S1**), with higher paleoproductivity values at the bottom of the core during the glacial period. The values rapidly decreased at approximately 15 kyrs BP until these proxies reached their minimum values at ~ 9 kyrs BP. However, a maximum value at approximately 4 kyrs BP, which was the transition between the Middle and Late Holocene, was observed in Core GL-1109 , in which *E. huxleyi* was the dominant species, accounting for approximately 70% of the total assemblage (**Figure 4G**).

Comparing these proxies with previous studies (**Figure 5**), we can observe that variation in the *F. profunda* percentage showed a similar trend to that for *G. sacculifer,* an oligotrophic foraminiferal species (Pereira et al., 2018), and an opposite distribution pattern to *G. bulloides* relative abundance (Pereira et al., 2018) and TOC content (Lourenço et al., 2016), demonstrating similar observations between the studies.

5 DISCUSSION

5.1 Sedimentary Processes as a Function of Sea-Level Variations

5.1.1 Similarity Among XRF, $CaCO_3$, and FF

According to the sedimentary record, it is possible to distinguish three different periods in both cores: the glacial period with a higher terrigenous supply, a brief transition period, and the Holocene with a lower terrigenous supply.

The FF positively correlated with the terrigenous sediment supply proxies (**Figures 3A–F**; **Tables 3**, **4**). The highest percentage of the FF occurred when sea level dropped. In contrast, the carbonate content had an opposite correlation and distribution with the FF (**Figures 3E–H**; **Tables 3**, **4**). Through these distributions, we can infer that the abundance of coccoliths did not cause changes in the FF. The primary process involved in these changes in the FF was the contribution of external silt–clay minerals associated with terrigenous supply, as observed by Costa et al. (2016).

The elementary ratio data show that the terrigenous sediment supply was maximal during the LGM (**Figures 3A–D**). This more significant terrigenous sediment supply possibly caused a dilution in the carbonate content values because they were minimal despite the higher paleoproductivity (**Figures 6C–H**), which was also observed by Arz et al. (1998) and Mahiques et al. (2007). After the end of the LGM, at approximately 19 kyrs BP, the terrigenous supply started to decline in the same proportion as the FF. An increase in the coarse fraction could indicate more marine influence ($CaCO_3$) or an increase in primary productivity because foraminiferal tests were the main component of this fraction. Both processes were observed in this period (**Figures 3C–H**), suggesting that deglaciation was a transition period of abrupt changes in the environment and deposition of sediments.

During the Holocene, the variability in terrigenous supply was stable compared to the differences between glacial and interglacial periods (**Figures 3A–D**). The stability tendency of carbonate variation (**Figures 3G,H**), even with variable biological productivity (**Figures 6E–H**), particularly in CoreGL-1109, also indicates that terrigenous sediments diluted the carbonate content.

The processes behind these observations may have been the variations in sea level and/or precipitation rates, which would have interfered with the riverine input and consequently in terrigenous supply and primary productivity, allowing a higher concentration of coarse fraction organisms. Analyzing the paleoproductivity record, we observed less productivity during this period (**Figures 6E–H**); therefore, we infer that a combined effect of sea level and precipitation was probably the main reason for changes in terrigenous input, FF and $CaCO_3$ content.

5.1.2 Main Sedimentary Process Drivers

The proxies for terrigenous sediment supply may vary mainly due to three processes. The first is relative sea-level variation. Its rise would make the transport of sediments to the upper continental slope more complicated since it would increase the distance between the core area and the sediment source, covering the shelf (Mahiques et al., 2004; Nagai et al., 2010). The second might be variation in fluvial discharge. In other words, with more precipitation, a higher terrigenous sediment supply would lead to higher values of these proxies during humid periods (Behling et al., 2000; Costa et al., 2016). The third might be percentage dilution of the continental material due to mixing with biogenic marine particles/material.

TABLE 3 | Correlation matrix (Pearson linear correlation coefficient, r) between all variables estimated in this study for the GL-824 core. Bold values correspond to a significant correlation at the 0.05 level.

	ln Ti/Ca	ln Fe/Ca	% $CaCO_3$	% FF	*E. huxleyi*	*F. profunda*	*Gephyrocapsa* spp.	Subtropical	N ratio	EPP
ln Ti/Ca	—	0.942	**-0.477**	**0.627**	**–0.522**	–0.133	**0.486**	**–0.266**	0.132	0.160
ln Fe/Ca	**0.942**	—	**-0.503**	**0.548**	**–0.484**	–0.126	**0.459**	**–0.277**	0.128	0.141
% $CaCO_3$	**–0.477**	**–0.503**	—	–0.172	**0.430**	–0.053	**-0.357**	**0.210**	0.043	0.077
% FF	**0.627**	**0.548**	**–0.172**	—	**-0.632**	–0.129	**0.551**	–0.085	0.114	0.166
E. huxleyi	**–0.522**	**–0.484**	**0.430**	**–0.632**	—	**0.217**	**-0.898**	0.152	**–0.203**	**–0.252**
F. profunda	–0.133	–0.126	–0.053	–0.129	0.217	—	**-0.601**	0.152	**–0.998**	**–0.971**
Gephyrocapsa spp.	**0.486**	**0.459**	**–0.357**	**0.551**	**–0.898**	**–0.601**	—	**–0.274**	**0.597**	**0.615**
Subtropical	**–0.266**	**–0.277**	**0.210**	–0.085	0.152	0.152	–0.274	—	**–0.188**	–0.158
N ratio	0.132	0.128	0.043	0.114	**–0.203**	**–0.998**	**0.597**	–0.188	—	**0.966**
EPP	0.160	0.141	0.077	0.166	–0.252	**–0.971**	**0.615**	–0.158	**0.966**	—

TABLE 4 | Correlation matrix (Pearson linear correlation coefficient, r) between all variables estimated in this study for the GL-1109 core. Bold values correspond to a significant correlation at the 0.05 level.

	ln Ti/Ca	ln Fe/Ca	% $CaCO_3$	% FF	*E. huxleyi*	*F. profunda*	*Gephyrocapsa* spp.	Subtropical	N ratio	EPP
ln Ti/Ca	—	**0.985**	**–0.798**	**0.809**	**–0.571**	**–0.359**	**0.708**	**0.183**	**0.359**	**0.313**
ln Fe/Ca	**0.985**	—	**–0.738**	**0.842**	**–0.519**	**–0.377**	**0.665**	**0.229**	**0.372**	**0.328**
% $CaCO_3$	**–0.798**	**–0.738**	—	**–0.564**	**0.551**	**0.307**	**–0.701**	–0.009	**–0.328**	**–0.295**
% FF	**0.809**	**0.842**	**–0.564**	—	**–0.308**	**–0.504**	**0.573**	0.255	**0.498**	**0.448**
E. huxleyi	**–0.571**	**–0.519**	**0.551**	**–0.308**	—	–0.137	**–0.736**	0.052	0.130	0.147
F. profunda	**–0.359**	**–0.377**	**0.307**	**–0.504**	–0.137	—	**–0.534**	–0.136	**–0.996**	**–0.989**
Gephyrocapsa spp.	**0.708**	**0.665**	**–0.701**	**0.573**	**–0.736**	**–0.534**	—	–0.094	**0.557**	**0.523**
Subtropical	**0.183**	**0.229**	–0.009	0.255	0.052	–0.136	–0.094	—	0.076	0.114
N ratio	**0.359**	**0.372**	**–0.328**	**0.498**	0.130	**–0.996**	**0.557**	0.076	—	**0.987**
EPP	**0.313**	**0.328**	**–0.295**	**0.448**	0.147	**–0.989**	**0.523**	0.114	**0.987**	—

The terrigenous supply had maximum values during the LGM when sea level reached its lowest position (**Figures 6C,D,I**). This indicates that a major continental shelf area was exposed, resulting in a more extensive area for weathering and a smaller distance between the sediment source and the study sites. Therefore, the continental slope was more likely to receive terrigenous sediments. Thus, the lower relative sea level contributed to more intense deposition of terrigenous and FF sediments (**Figures 3E,F** and **Figure 6I**). This could also have been connected to the offshore displacement of the BC to deeper regions during the LGM (Viana et al., 1998; Mahiques et al., 2007; Kowsmann et al., 2015), which would have lowered the local hydrodynamics and allowed or enhanced the deposition of FF sediments.

There was a stable sea level during the Holocene. Nevertheless, the input of terrigenous sediments showed a slight increase. This was linked to an increase in rainfall that occurred during this period (**Figures 6C,D,I,J**), suggesting that precipitation was directly responsible for these oscillations during this specific period.

Wang et al. (2007) analyzed precipitation during the study period based on $\delta^{18}O$ data from speleothems. These data showed variability similar to the variation in the FF (**Figures 3E,F** and **Figure 6J**), especially in GL-824 core, probably because the primary source of fine sediments was fluvial runoff, which was higher when precipitation rates were higher. According to Behling et al. (2000), when there are periods with more precipitation, there are increases in the Fe/Ca and Ti/Ca ratio values. This was also observed in our study (**Figures 6C,D,J**). In other words, precipitation can be a controlling factor in the terrigenous supply. During the LGM, humidity was higher in South America than during the Holocene (Cruz et al., 2005; Wang et al., 2007; Sylvestre, 2009); therefore, fluvial runoff would have been higher thus transporting more terrigenous sediments to the continental slope. According to Jennerjahn et al. (2004) and Jaeschke et al. (2007), this increase in precipitation was related to the displacement of the ITCZ to the south and an increase in the intensity of winds from the southeast during colder periods, also increasing the humidity on the continent.

Comparing the precipitation oscillation to the paleoproductivity and terrigenous supply proxies, we observed that the general trend was similar between these indicators (**Figures 6C–J**). However, when precipitation had higher peaks without substantial sea-level variation, we did not observe significant changes in any other proxies, highlighting that rainfall may have influenced terrigenous supply and FF records, but on a smaller scale. The moisture source can also influence the $\delta^{18}O$ speleothems record and not only the precipitation intensity (Lee et al., 2009). Furthermore, there are differences between LGM rainfall reconstructed by nonisotope proxies and interpretations of speleothem records

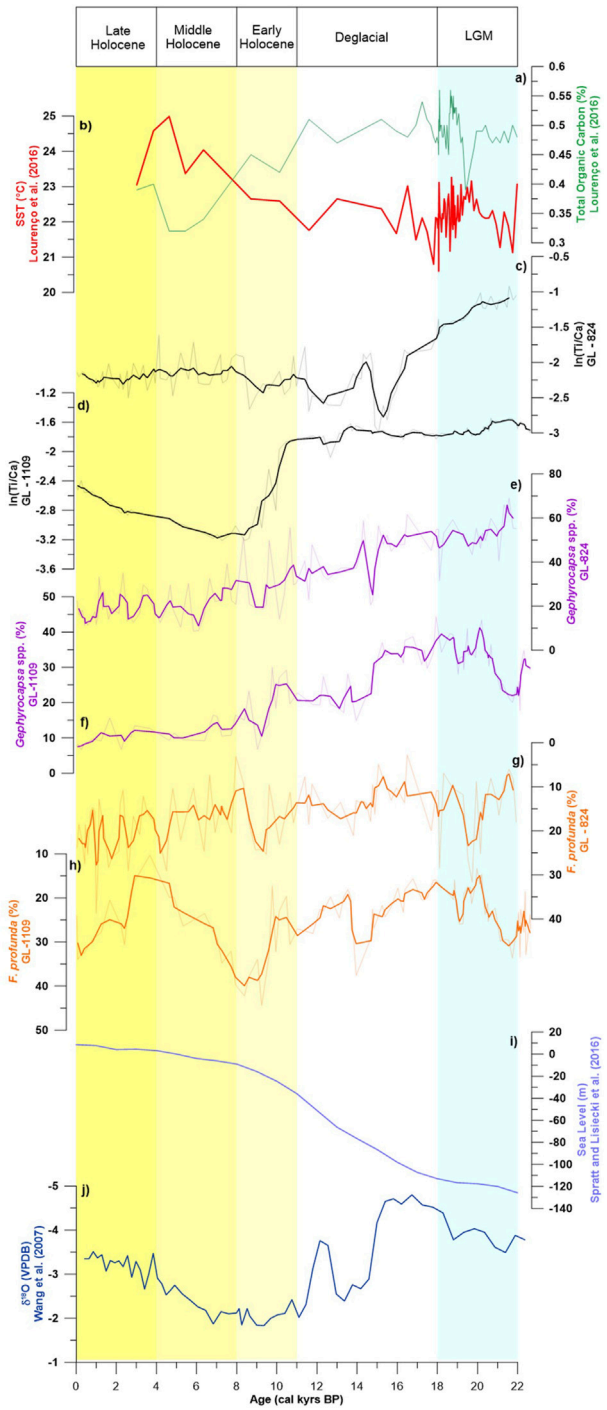

FIGURE 6 | Comparison of the results obtained in GL-824 and GL-1109 with those of other studies. Thick lines represent a weighted average of 3 points, and the background lines are the original data. **(A)** Total organic carbon and **(B)** sea surface temperature calculated based on alkenones (Lourenço et al., 2016). Measured ln (Ti/Ca) for **(C)** GL-824 and **(D)** GL-1109. The relative abundance of eutrophic *Gephyrocapsa* spp. for **(E)** GL-824 and **(F)** GL-1109. Relative abundance of the oligotrophic proxy *F. profunda* for **(G)** GL-824 and **(H)** GL-1109. **(I)** Sea-level reconstruction (Spratt and Lisiecki, 2016). **(H)** Oxygen isotope composition of speleothems in the Botuverá cave (Wang et al., 2007).

(Sylvestre, 2009; Berman et al., 2016). Thus, we interpreted the maximum terrigenous supply to the upper slope during the glacial period to have been primarily due to the effects of lower sea level. Besides, the possible rise in precipitation could also be improving the terrigenous supply.

Several researchers have previously observed the influence of Heinrich events in the Southern Hemisphere in the tropical region of the South Atlantic (Arz et al., 1999; Vidal et al., 1999; Jennerjahn et al., 2004; Jaeschke et al., 2007), yet in our study, we did not observe a significant influence of Heinrich events or even of the Younger Dryas (**Figures 6C,D**). These events could have led to the movements of the ITCZ, causing anomalously higher precipitation rates in southeastern Brazil (Cruz et al., 2006; Wang et al., 2007). This should have raised fluvial runoff, transporting more terrigenous sediments and nutrients to the core region. Nevertheless, we did not observe such changes in either of these records, indicating that the main driver of most changes in the deposition of terrigenous sediments was probably relative sea-level variation (**Figure 7**).

Changes in sedimentary proxies can also indicate changes in the hydrodynamics of the region. A low-energy environment would allow more deposition of silt–clay minerals than a high-energy environment. This process has already been correlated with the displacement of the BC toward the coast, which resulted from the higher relative sea-level conditions and the covering of the continental shelf, as has also been described by other authors (Viana et al., 1998; Mahiques et al., 2007; Kowsmann 2015). The offshore displacement of the BC system can lead to more fine sediments depositing on the upper slope (Viana et al., 1998; Mahiques et al., 2007; Nagai et al., 2010; Kowsmann et al., 2015). This displacement would diminish the local hydrodynamics and promote the deposition of the FF. Furthermore, the "floor polisher" effect on the seabed described by Mahiques et al. (2004) would prevent mud deposition on the shelf break and upper slope depths in the periods where the BC moved toward the coast.

The XRF and FF records of the two cores have different trends. GL-824 shows a decrease over the last deglaciation, while GL-1109 remains constant. The decreasing trend in GL-1109 is observed during the early Holocene. Additionally, in GL-824 core, there was a more significant amount of FF and terrigenous sediments and lower percentages of $CaCO_3$ than in GL-1109 core (**Figures 3E–H**), highlighting differences in sedimentary processes between the two cores. This is primarily associated with their different water depths (**Figure 1B**). GL-824 location is more susceptible to sea-level variations because this core is located on the upper slope, an environment that during the LGM would be analog to the continental shelf. Consequently, the coastal processes influence more the GL-824 than the GL-1109. Thus, its elements and granulometry change as soon as the sea level rises. On the other hand, in the GL-1109, the trends of the terrigenous supply and FF occur later when the sea level is nearly at its maximum. GL-824 core would also have been less affected by the action of the BC compared with GL- 1109. Moreover, GL-824 core is farther north than GL-

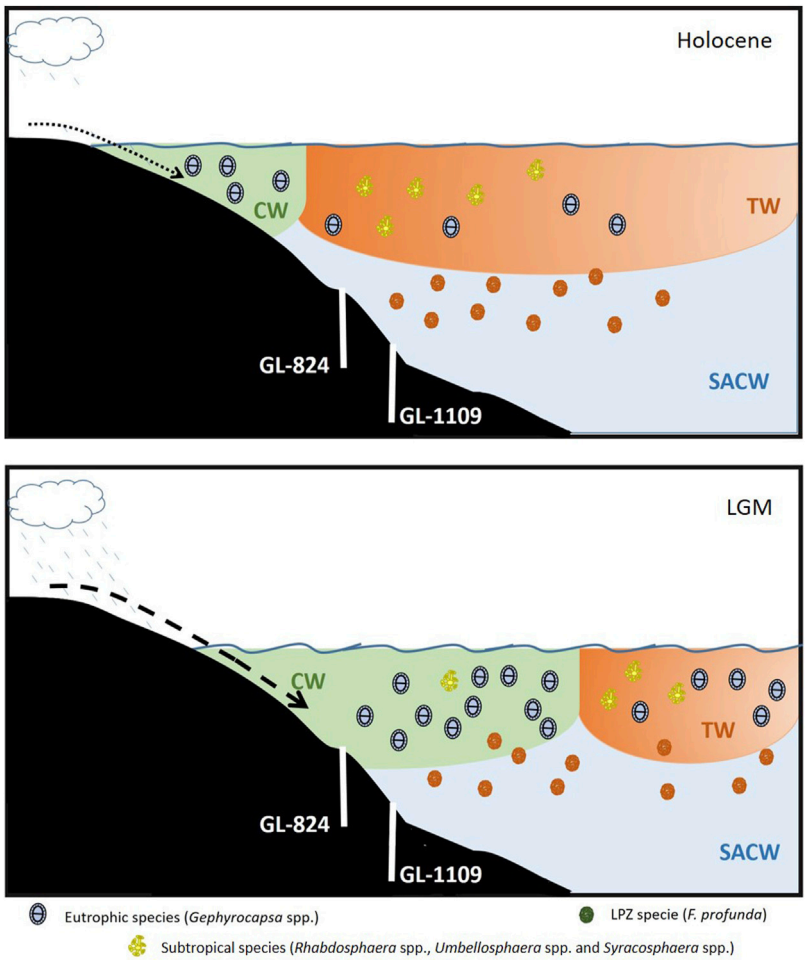

FIGURE 7 | Conceptual model of the main processes controlling the terrigenous supply and paleoproductivity in the southwestern Atlantic. The model shows high (low) productivity during the LGM (Holocene) period on the upper slope associated with variations in sea level and precipitation, promoting more input of nutrients due to enhanced terrigenous supply caused by a combination of lower sea level and higher rainfall. At the same time, the offshore displacement of the BC occurred, increasing the influence of the more eutrophic CW in the core area during the LGM.

1109 core, placing it closer to sediment sources such as Rio Doce and Rio Paraíba do Sul.

5.2 Coccolithophore Response to Paleoproductivity Variations in the Southwestern Atlantic Ocean

5.2.1 Coccolithophore Assemblage Response

The relative abundance of *F. profunda* was opposite to the total organic carbon (TOC) content (Lourenço et al., 2016) and the *G. bulloides* percentage (Pereira et al., 2018). Additionally, it was similar to higher SSTs (Lourenço et al., 2016) and the relative abundance of the oligotrophic *G. sacculifer* (**Figures 5A–I**, Pereira, et al., 2018). Therefore, we used this species to indicate oligotrophic conditions, which has also been corroborated by other studies (Beaufort et al., 2001; Hernandez-Almeida et al., 2019).

Emiliania huxleyi and *F. profunda* showed a similar general fluctuation (**Figures 5A–D**). *E. huxleyi* is known to tolerate a wide range of ecological conditions (Okada and Honjo, 1973; Okada and McIntyre, 1979; Boeckel and Baumann, 2008) and can dominate in both oligotrophic (Okada and Honjo, 1975; Kleijne, 1993; Haidar and Thierstein, 2001; Tyrrell and Merico, 2004) and eutrophic environments (Brand, 1994; Young, 1994; Boeckel et al., 2006). In contrast, *Gephyrocapsa* spp. exhibits an inverse distribution compared to *F. profunda* (**Figures 5A–F**; **Tables 3**, **4**), indicating the different environmental preferences of these species. In the Iberian margin upwelling region, *E. huxleyi* and *Gephyrocapsa* spp (mainly small *Gephyrocapsa* and *G. oceanica*) were both indicators of upwelling periods (Ausín et al., 2018). However, they were separated into distinct ecological preferences, with *E. huxleyi* related to a more stable, warmer, and nutrient-poor water column associated with the upwelling relaxation stage and *Gephyrocapsa* spp. to colder water and higher nutrient availability associated with the early stages of the upwelling event (Ausín et al., 2018; Jin et al. (2019) in the South China Sea also found that *Gephyrocapsa* spp. were dominant in coastal water associated with

higher diatom production and increased silicon content, while *E. huxleyi* was associated with a regular nutrient regime with lower amounts of silicon.

Comparing our record to SSTs estimated by Lourenço et al. (2016), we analyzed the same process described by Jin et al. (2019), with *E. huxleyi* dominating the period with warm and stable water and *Gephyrocapsa* spp. with colder nutrient-rich (silicon) water of the CW (**Figures 5C–F** and **Figures 6B–F**). Additionally, *E. huxleyi* had higher abundances in the periods with lower riverine influence, more negligible rainfall, and higher sea level, interpreted here as a low nutrient period, which was similar to *F. profunda* and the subtropical species that are associated with high temperature and oligotrophic environments (Boeckel et al., 2006). In this work, we interpreted the variations in *E. huxleyi* with a possible relation to more oligotrophic environments and as a response to evolutionary factors. This species first appeared and rapidly grew in the late/middle Quaternary, replacing the former more abundant *Gephyrocapsa* spp. (Toledo et al., 2016), making it a species with a signal that is difficult to deduce. Furthermore, as a cosmopolitan species, it may not indicate upwelling processes but is more typical of a stable regime, as observed in other studies (Andruleit and Rogalla, 2002; Jin et al., 2019).

Since *Gephyrocapsa* spp. and *E. huxleyi* seem to represent different ecological aspects, the N ratio (Flores et al., 2000) is not the best proxy to estimate paleoproductivity in this region. Therefore, the leading proxy used in this study to infer changes in primary productivity in surface water was the contrast between eutrophic *Gephyrocapsa* spp. and *F. profunda*, which represents low nutrients in surface water.

Variations in the relative abundances of *F. profunda* and *Gephyrocapsa* spp., particularly in GL-1109, were very similar to TOC content and *G. bulloides* relative abundance (**Figures 5A–H**), showing higher nutrients/productivity during the glacial period and lower nutrients/productivity during the Holocene, with a transition period of ~19 kyrs BP to ~14 kyrs BP. These observed variations likely reflect the opposite trend in the relative abundances of *F. profunda* and *Gephyrocapsa* spp., which reveals a change in the upper water column during these periods, with the LGM period characterized by a shallower nutricline and high productivity and the interglacial period characterized by a deeper nutricline and lower productivity. This is also supported by the UPZ species in the subtropical group, an indicator of oligotrophic surface environments, being more abundant in the Holocene than in the LGM, suggesting a warmer and poor-nutrient surface ocean during the Holocene. Nagai et al. (2010), mainly applying benthic foraminifera, and Mahiques et al. (2007), using sedimentary data, also inferred high productivity during the LGM on the southeastern Brazilian upper slope. Toledo et al. (2008) reported evidence of decreased productivity over the Holocene compared to the LGM along the Brazilian continental margin, which is consistent with our observations.

The terrigenous supply and FF content oscillated similarly to the *Gephyrocapsa* spp. record, in contrast to the subtropical group (**Tables 3**, **4**). Three processes could lead to this configuration, or a combination of all of them: 1) there was high availability of nutrients in the UPZ during the low stands of sea level, caused by a higher riverine input transporting more nutrients along with terrigenous material. 2) Higher influence of coastal nutrient-rich water due to the offshore displacement of the BC during low stands of sea level, leading to withdrawal of the surface warm oligotrophic TW (**Figure 7**). 3) High turbidity in the UPZ due to higher FF content and terrigenous sediments in the water column decreasing the light availability to the LPZ, limiting the growth of *F. profunda*.

5.2.2 Productivity Driving Factors in the Southwestern Atlantic

Gephyrocapsa spp. and EPP indicators reflect the same three distinct periods noted in the geochemical and sedimentary record. This suggests that a more substantial continental influence or the BC offshore displacement during the glacial period would have enhanced nutrient availability in surface water. In the same way, during the LGM, a weaker BC would have had more eddies and meanders because stronger currents were closer to linear fluxes. These meanders could have transported more nutrients to the photic zone from greater depths if they were anticyclones or by mixing ocean water with shelf water, which contains higher nutrient concentrations. The Plata River plume could also have reached the study area more frequently during winter-like conditions, promoting higher nutrients and terrigenous input.

Guerreiro et al. (2013) observed a more significant presence of *G. oceanica* in the water column associated with higher productivity related to fluvial discharge on the central Portuguese margin. Mahiques et al. (2007) and Nagai et al. (2010) suggested an increase in water column temperature and more intense action of the BC during periods of higher sea level, indicating a displacement of the warm water of the Brazil Current toward the coast, which would have prevented any increase in water productivity or the deposition of organic matter.

The correlation between the terrigenous supply, productivity, and nutrient content in surface water, represented by *Gephyrocapsa* spp. (**Table 2**), can be explained by two factors: 1) there was probably high nutrient content in the water column transported by enhanced continental runoff during lowstands of sea level and more winter-like conditions increasing the influence of the Plata River plume (Portilho-Ramos et al., 2019); and 2) the displacement of the BC toward the coast during higher sea level enhanced the influence of the TW, transporting more oligotrophic water, deepening the nutricline and preventing any increase in nutrient content (**Figure 7**). This shows that in the study region, *Gephyrocapsa* spp. is a more opportunistic species than *E. huxleyi*, especially when there is a more substantial influence of coastal water because *G. oceanica* tends to dominate such regions (Guerreiro et al., 2013; Ausín et al., 2018). Furthermore, all processes could act simultaneously, increasing continental runoff related to enhanced rainfall (Wang et al., 2007) and favorable conditions for the northward penetration of the Plata River plume, as also suggested by Portilho-Ramos et al. (2019).

During periods of lower sea level, the input of nutrients and terrigenous materials favored the productivity and deposition of organic carbon (**Figures 6A–I**), which was observed by Lourenço et al. (2016). Lower $CaCO_3$ content corresponded to the period of higher SSTs, productivity, and terrigenous supply (**Figures 3G,H** and **Figures 6A–H**), which demonstrates an inverse correlation

between the productivity record and carbonate content (**Tables 3**, **4**), suggesting a possible dilution effect of the carbonate content by terrigenous input. Along with this dilution during periods of higher terrigenous input, there was an increase in FF content, increasing turbidity and lowering light penetration in the LPZ, limiting the growth of *F. profunda* and enhancing the relative abundance of the UPZ dweller *Gephyrocapsa* spp.

The deglacial transitional period was characterized by a decrease in paleoproductivity and terrigenous supply (**Figures 6C–H**). This was probably related to the processes discussed above (i.e., sea level rise and diminished precipitation), both limiting the nutrient input to the study area from both sources: continental input (regional input or lower Plata River plume influence) and the closer BC system increasing the oligotrophic TW influence. In addition, sea level rise may have modified the region's geomorphology, limiting shelf-break upwelling to areas closer to the coast.

As stated before, the Holocene was a period with the lowest productivity. However, the transition between the Middle to Late Holocene had low percentages of *F. profunda* (EPP, **Supplementary Material**) in the GL-1109 core (**Figure 6H**). This was not related to precipitation or sea-level oscillation because these parameters were relatively stable during this period. The low *F. profunda* relative abundance was caused by the higher relative abundances of *E. huxleyi*, representing approximately 70% of the assemblage during this period (**Figure 5D**). Most likely, related to changes in sea surface nutrients, also in the same interval, we observed high percentages of the eutrophic indicator *Helicosphaera* spp. (Boeckel et al., 2006) and lower rates of oligotrophic *Umbellosphaera* spp. (Boeckel et al., 2006; Saavedra-Pelitero et al., 2011) and subtropical groups (**Supplementary Figure S2**). Austral summer-like conditions observed in the Middle-Late Holocene could have promoted increased shelf-break upwelling, which would have been enhanced due to higher BC meander-driven upwelling, causing higher rates of primary productivity in more offshore positions affecting the GL-1109 region, but not the shallower GL-824 core, which would have been influenced by colder coastal water and did not show such peaks in *E. huxleyi* relative abundance.

6 CONCLUSION

The distribution of terrigenous proxies, together with the fine fraction and carbonate contents, represented good indicators of the transport of sediments to the upper continental slope.

The terrigenous supply varied between the LGM and the Holocene, with the relative sea-level being the central controller and precipitation possibly enhancing this supply. Sea-level fluctuations were responsible for determining the distance between the sediment source and the core area and modulating how the BC displacement influenced sediment deposition. Therefore, the terrigenous supply was higher during the LGM, when sea level was lower and precipitation rates were higher. The BC dislocated offshore also led to a less energetic environment promoting the deposition of the fine fraction and terrigenous sediments.

The paleoproductivity of the upper slope was controlled mainly by the position of the BC main flow, which was associated with relative sea level. In the Holocene, a period of high sea level, the BC transports warm water of the TW to the upper slope, preventing any nutrient arrival, which was opposite to that during the LGM, an interval with lower sea level in which offshore displacement of the BC allowed the transport of more nutrients, enhancing primary productivity. Similar associations of this process have been made based on different proxies (Mahiques et al., 2007; Nagai et al., 2010; Lourenço et al., 2016), but this is the first study based on coccolithophores from the LGM-Holocene transition in the southwestern Atlantic.

DATA AVAILABILITY STATEMENT

The original contributions presented in the study are included in the article/**Supplementary Materials**; further inquiries can be directed to the corresponding author.

AUTHOR CONTRIBUTIONS

GP: writing—original draft, and geochemical analysis. MH: coccolithophore assemblages and review and editing. MT: conceptualization, investigation, and writing—review and editing. AA: conceptualization and writing—review and editing. CC: conceptualization and writing—review and editing. KC: supervision, project administration, and writing—review and editing. FT: supervision, project administration, funding acquisition, and writing—review and editing.

FUNDING

This study was supported by the CAPES-ASPECTO project (grant no. 88887.091731/2014-01). GAP acknowledges the financial support from CNPq (grant 167794/2018-3). MOT appreciates financial support from Capes (grant 88887.388307/2019-00). ALSA is a senior scholar CNPq (grant 302521/2017-8). CMC acknowledges the financial support from FAPESP (grants 2018/15123-4 and 2019/24349-9) and CNPq (grant 312458/2020-7). KBC acknowledges the financial support from CNPq (grant 310909/2019-8). FALT appreciates financial support from CNPq (310843/2019-7).

ACKNOWLEDGMENTS

The authors wish to express their thanks to R. Kowsman (CENPES/Petrobras) and the Petrobras Core Repository staff (Macaé/Petrobras) for providing the sediment core used in this research. Acknowledgments are also due to the reviewers for their insightful suggestions.

SUPPLEMENTARY MATERIAL

The Supplementary Material for this article can be found online at: https://www.frontiersin.org/articles/10.3389/feart.2022.846245/full#supplementary-material

REFERENCES

Alves, E., Macario, K., Souza, R., Pimenta, A., Douka, K., Oliveira, F., et al. (2015). Radiocarbon Reservoir Corrections on the Brazilian Coast from Pre-bomb Marine Shells. *Quat. Geochronol.* 29, 30–35. doi:10.1016/j.quageo.2015.05.006

Andruleit, H., and Rogalla, U. (2002). Coccolithophores in Surface Sediments of the Arabian Sea in Relation to Environmental Gradients in Surface Waters. *Mar. Geol.* 186 (3-4), 505–526. doi:10.1016/S0025-3227(02)00312-2

Antunes, R. L. (1997). *Introdução Ao Estudo Dos Nanofósseis Calcários*. Rio de Janeiro: Instituto de Geociências-Universidade Federal do Rio de Janeiro.115

Arz, H. W., Pätzold, J., and Wefer, G. (1999). Climatic Changes during the Last Deglaciation Recorded in Sediment Cores from the Northeastern Brazilian Continental Margin. *Geo-Marine Lett.* 19 (3), 209–218. doi:10.1007/s003670050111

Arz, H. W., Pätzold, J., and Wefer, G. (1998). Correlated Millennial-Scale Changes in Surface Hydrography and Terrigenous Sediment Yield Inferred from Last-Glacial Marine Deposits off Northeastern Brazil. *Quat. Res.* 50 (2), 157–166. doi:10.1006/qres.1998.1992

Ausín, B., Zúñiga, D., Flores, J. A., Cavaleiro, C., Froján, M., Villacieros-Robineau, N., et al. (2018). Spatial and Temporal Variability in Coccolithophore Abundance and Distribution in the NW Iberian Coastal Upwelling System. *Biogeosciences* 15 (1), 245–262. doi:10.5194/bg-15-245-2018

Beaufort, L., de Garidel-Thoron, T., Mix, A. C., and Pisias, N. G. (2001). ENSO-like Forcing on Oceanic Primary Production during the Late Pleistocene. *Science* 293 (5539), 2440–2444. doi:10.1126/science.293.5539.2440

Beaufort, L., Lancelot, Y., Camberlin, P., Cayre, O., Vincent, E., Bassinot, F., et al. (1997). Insolation Cycles as a Major Control of Equatorial Indian Ocean Primary Production. *Science* 278 (5342), 1451–1454. doi:10.1126/science.278.5342.1451

Behling, H. (2002). South and Southeast Brazilian Grasslands during Late Quaternary Times: a Synthesis. *Palaeogeogr. Palaeoclimatol. Palaeoecol.* 177 (1-2), 19–27. doi:10.1016/S0031-0182(01)00349-2

Behling, H., W. Arz, H., Pätzold, J., and Wefer, G. (2000). Late Quaternary Vegetational and Climate Dynamics in Northeastern Brazil, Inferences from Marine Core GeoB 3104-1. *Quat. Sci. Rev.* 19 (10), 981–994. doi:10.1016/S0277-3791(99)00046-3

Berman, A. L., Silvestri, G. E., and Tonello, M. S. (2016). Differences between Last Glacial Maximum and Present-Day Temperature and Precipitation in Southern South America. *Quat. Sci. Rev.* 150, 221–233. doi:10.1016/j.quascirev.2016.08.025

Bícego, M. C., Santos, F. R., de Aandrade Furlan, P. C., Lourenço, R. A., Taniguchi, S., de Mello e Sousa, S. H., Nagai, R. H., Cavalcante, A. B. L., Figueira, R. C. L., Wainer, I. K. C., and de Mahiques, M. M. (2021). Mid- to Late-Holocene Analysis of the Influence of the La Plata River Plume on the Southwestern Atlantic Shelf: A Paleoenvironmental Reconstruction Based on Lipid Biomarkers and Benthic Foraminifera. *Holocene* 095968362110417. doi:10.1177/09596836211041727

Blaauw, M., and Christen, J. A. (2011). Flexible Paleoclimate Age-Depth Models Using an Autoregressive Gamma Process. *Bayesian Anal.* 6, 457–474. doi:10.1214/11-BA61810.1214/ba/1339616472

Boeckel, B., and Baumann, K.-H. (2004). Distribution of Coccoliths in Surface Sediments of the South-Eastern South Atlantic Ocean: Ecology, Preservation and Carbonate Contribution. *Mar. Micropaleontol.* 51 (3-4), 301–320. doi:10.1016/j.marmicro.2004.01.001

Boeckel, B., Baumann, K.-H., Henrich, R., and Kinkel, H. (2006). Coccolith Distribution Patterns in South Atlantic and Southern Ocean Surface Sediments in Relation to Environmental Gradients. *Deep Sea Res. Part I Oceanogr. Res. Pap.* 53 (6), 1073–1099. doi:10.1016/j.dsr.2005.11.006

Boeckel, B., and Baumann, K.-H. (2008). Vertical and Lateral Variations in Coccolithophore Community Structure across the Subtropical Frontal Zone in the South Atlantic Ocean. *Mar. Micropaleontol.* 67 (3-4), 255–273. doi:10.1016/j.marmicro.2008.01.014

Bradley, R. S. (2000). Past Global Changes and Their Significance for the Future. *Quat. Sci. Rev.* 19 (1-5), 391–402. doi:10.1016/S0277-3791(99)00071-2

Brand, L. E. (1994). "Physiological Ecology of Marine Coccolithophores," in *Coccolithophores*. Editors A. Winter and W. G. Siesser (Cambridge: Cambridge University Press), 39

Cabarcos, E., Flores, J.-A., and Sierro, F. J. (2014). High-resolution Productivity Record and Reconstruction of ENSO Dynamics during the Holocene in the Eastern Equatorial Pacific Using Coccolithophores. *Holocene* 24 (2), 176–187. doi:10.1177/0959683613516818

Campos, E. J. D., Gonçalves, J. E., and Ikeda, Y. (1995). Water Mass Characteristics and Geostrophic Circulation in the South Brazil Bight: Summer of 1991. *J. Geophys. Res. Oceans* 100 (C9), 18537–18550. doi:10.1029/95JC01724

Campos, E. J. D., Lentini, C. A. D., Miller, J. L., and Piola, A. R. (1999). Interannual Variability of the Sea Surface Temperature in the South Brazil Bight. *Geophys. Res. Lett.* 26 (14), 2061–2064. doi:10.1029/1999GL900297

Campos, E. J. D., Velhote, D., and da Silveira, I. C. A. (2000). Shelf Break Upwelling Driven by Brazil Current Cyclonic Meanders. *Geophys. Res. Lett.* 27 (6), 751–754. doi:10.1029/1999GL010502

Carvalho, L. M. V., Jones, C., and Liebmann, B. (2002). Extreme Precipitation Events in Southeastern South America and Large-Scale Convective Patterns in the South Atlantic Convergence Zone. *J. Clim.* 15 (17), 2377–2394. doi:10.1175/1520-0442(2002)015<2377:epeiss>2.0.co;2

Carvalho, L. M. V., Jones, C., and Liebmann, B. (2004). The South Atlantic Convergence Zone: Intensity, Form, Persistence, and Relationships with Intraseasonal to Interannual Activity and Extreme Rainfall. *J. Clim.* 17 (1), 88–108. doi:10.1175/1520-0442(2004)017<0088:tsaczi>2.0.co;2

Cheng, H., Sinha, A., Cruz, F. W., Wang, X., Edwards, R. L., d'Horta, F. M., et al. (2013). Climate Change Patterns in Amazonia and Biodiversity. *Nat. Commun.* 4, 1411. doi:10.1038/ncomms2415

Ciotti, Á. M., Odebrecht, C., Fillmann, G., and Moller, O. O., Jr (1995). Freshwater Outflow and Subtropical Convergence Influence on Phytoplankton Biomass on the Southern Brazilian Continental Shelf. *Cont. shelf Res.* 15 (14), 1737–1756. doi:10.1016/0278-4343(94)00091-Z

Costa, K. B., Cabarcos, E., Santarosa, A. C. A., Battaglin, B. B. F., and Toledo, F. A. L. (2016). A Multiproxy Approach to the Climate and Marine Productivity Variations along MIS 5 in SE Brazil: A Comparison between Major Components of Calcareous Nannofossil Assemblages and Geochemical Records. *Palaeogeogr. Palaeoclimatol. Palaeoecol.* 449, 275–288. doi:10.1016/j.palaeo.2016.02.032

Cremer, M., Gonthier, E., Duprat, J., Faugères, J.-C., and Courp, T. (2007). Late Quaternary Variability of the Sedimentary Record in the Sao Tome Deep-Sea System (South Brazilian Basin). *Mar. Geol.* 236 (3-4), 223–245. doi:10.1016/j.margeo.2006.10.032

Cruz, F. W., Burns, S. J., Karmann, I., Sharp, W. D., Vuille, M., Cardoso, A. O., et al. (2005). Insolation-driven Changes in Atmospheric Circulation over the Past 116,000 Years in Subtropical Brazil. *Nature* 434 (7029), 63–66. doi:10.1038/nature03365

Cruz, F. W., Jr, Burns, S. J., Karmann, I., Sharp, W. D., and Vuille, M. (2006). Reconstruction of Regional Atmospheric Circulation Features during the Late Pleistocene in Subtropical Brazil from Oxygen Isotope Composition of Speleothems. *Earth Planet. Sci. Lett.* 248 (1-2), 495–507. doi:10.1016/j.epsl.2006.06.019

da Silveira, I. C. A., Napolitano, D. C., and Farias, I. U. (2020). "Water Masses and Oceanic Circulation of the Brazilian Continental Margin and Adjacent Abyssal Plain," in *Brazilian Deep-Sea Biodiversity*. Editors P. Y. G. Sumida, A. F. Bernardino, and F. C. D. Léo (Cham): Springer), 7–36. doi:10.1007/978-3-030-53222-2_2

de Mahiques, M. M., Tessler, M. G., Maria Ciotti, A., da Silveira, I. C. A., e Sousa, S. H. d. M., Figueira, R. C. L., et al. (2004). Hydrodynamically Driven Patterns of Recent Sedimentation in the Shelf and Upper Slope off Southeast Brazil. *Cont. Shelf Res.* 24 (15), 1685–1697. doi:10.1016/j.csr.2004.05.013

Dennison, J. M., and Hay, W. W. (1967). Estimating the Needed Sampling Area for Subaquatic Ecological Studies. *J. Paleontol.* 41 (3), 706

Deplazes, G., Lückge, A., Peterson, L. C., Timmermann, A., Hamann, Y., Hughen, K. A., et al. (2013). Links between Tropical Rainfall and North Atlantic Climate during the Last Glacial Period. *Nat. Geosci.* 6 (3), 213–217. doi:10.1038/ngeo1712

Fatela, F., and Taborda, R. (2002). Confidence Limits of Species Proportions in Microfossil Assemblages. *Mar. Micropaleontol.* 45, 169–174. doi:10.1016/s0377-8398(02)00021-x

Flores, J.-A., Gersonde, R., and Sierro, F. J. (1999). Pleistocene Fluctuations in the Agulhas Current Retroflection Based on the Calcareous Plankton Record. *Mar. Micropaleontol.* 37 (1), 1–22. doi:10.1016/S0377-8398(99)00012-2

Flores, J. A., Bárcena, M. A., and Sierro, F. J. (2000). Ocean-surface and Wind Dynamics in the Atlantic Ocean off Northwest Africa during the Last 140 000 Years. *Palaeogeogr. Palaeoclimatol. Palaeoecol.* 161 (3-4), 459–478. doi:10.1016/S0031-0182(00)00099-7

Govin, A., Braconnot, P., Capron, E., Cortijo, E., Duplessy, J.-C., Jansen, E., et al. (2012a). Persistent Influence of Ice Sheet Melting on High Northern Latitude Climate during the Early Last Interglacial. *Clim. Past.* 8, 483–507. doi:10.5194/cp-8-483-2012

Govin, A., Holzwarth, U., Heslop, D., Ford Keeling, L., Zabel, M., Mulitza, S., et al. (2012b). Distribution of Major Elements in Atlantic Surface Sediments (36°N-49°S): Imprint of Terrigenous Input and Continental Weathering. *Geochem. Geophys. Geosyst.* 13 (1), a–n. doi:10.1029/2011GC003785

Guerreiro, C., Oliveira, A., De Stigter, H., Cachão, M., Sá, C., Borges, C., et al. (2013). Late Winter Coccolithophore Bloom off Central Portugal in Response to River Discharge and Upwelling. *Cont. Shelf Res.* 59, 65–83. doi:10.1016/j.csr.2013.04.016

Haidar, A. T., and Thierstein, H. R. (2001). Coccolithophore Dynamics off Bermuda (N. Atlantic). *Deep Sea Res. Part II Top. Stud. Oceanogr.* 48 (8-9), 1925–1956. doi:10.1016/S0967-0645(00)00169-7

Hammer, O., Harper, D. A. T., and Ryan, P. D. (2001). Past: Paleontological Statistics Software Package for Education and Data Analysis. *Palaeontol. Electron* 4 (1), 1–9. http://palaeoelectronica.org/2001_1/past/issue1_01.htm.

Hernández-Almeida, I., Ausín, B., Saavedra-Pellitero, M., Baumann, K.-H., and Stoll, H. M. (2019). Quantitative Reconstruction of Primary Productivity in Low Latitudes during the Last Glacial Maximum and the Mid-to-late Holocene from a Global *Florisphaera Profunda* Calibration Dataset. *Quat. Sci. Rev.* 205, 166–181. doi:10.1016/j.quascirev.2018.12.016

Jaeschke, A., Rühlemann, C., Arz, H., Heil, G., and Lohmann, G. (2007). Coupling of Millennial-Scale Changes in Sea Surface Temperature and Precipitation off Northeastern Brazil with High-Latitude Climate Shifts during the Last Glacial Period. *Paleoceanography* 22, 4, a–n. doi:10.1029/2006PA001391

Jansen, J. H., van der Gaast, S. J., Koster, B., and Vaars, A. J. (1998). CORTEX, a Shipboard XRF Scanner for Element Analyses in Split Sediment Cores. *Mar. Geol.* 151 (1), 143–153. doi:10.1016/S0025-3227(98)00074-7

Jennerjahn, T. C., Ittekkot, V., Arz, H. W., Behling, H., Pätzold, J., and Wefer, G. (2004). Asynchronous Terrestrial and Marine Signals of Climate Change during Heinrich Events. *Science* 306 (5705), 2236–2239. doi:10.1126/science.1102490

Jin, X. B., Liu, C. L., Zhao, Y. L., Zhang, Y. W., Wen, K., Lin, S., et al. (2019). Two Production Stages of Coccolithophores in Winter as Revealed by Sediment Traps in the Northern South China Sea. *J. Geophys. Res. Biogeosci.* 124 (7), 2335–2350. doi:10.1029/2019JG005070

Kleijne, A. (1993). "*Morphology, Taxonomy and Distribution of Extant Coccolithophorids (Calcareous Nannoplankton)*. Amsterdam: Free University of Amsterdam). thesis.

Kowsmann, R. O., de Lima, A. C., and Vicalvi, M. A. (2015). "Feições Indicadoras De Instabilidade Geológica No Talude Continental E No Platô De São Paulo," in *Geologia e Geomorfologia* (Campus, 71–97. doi:10.1016/B978-85-352-6937-6.50012-4

Lee, J.-E., Johnson, K., and Fung, I. (2009). Precipitation over South America during the Last Glacial Maximum: An Analysis of the "amount Effect" with a Water Isotope-Enabled General Circulation Model. *Geophys. Res. Lett.* 36, L19701. doi:10.1029/2009GL039265

Leonhardt, A., Toledo, F. A. L., and Coimbra, J. C. (2013). The Productivity History in the Southwestern Atlantic as Inferred from Coccolithophore Record for the Last 130 Kyr. *Rev. Bras. Paleontol.* 16 (3), 361–375. doi:10.4072/rbp.2013.3.02

Liebmann, B., Vera, C. S., Carvalho, L. M. V., Camilloni, I. A., Hoerling, M. P., Allured, D., et al. (2004). An Observed Trend in Central South American Precipitation. *J. Clim.* 17 (22), 4357–4367. doi:10.1175/3205.1

Locarnini, M. M., Mishonov, A. V., Baranova, O. K., Boyer, T. P., Zweng, M. M., Garcia, H. E., et al. (2018). World Ocean Atlas 2018. *Temperature* 1, 52.

Lourenço, R. A., de Mahiques, M. M., Wainer, I. E. K. C., Rosell-Melé, A., and Bícego, M. C. (2016). Organic Biomarker Records Spanning the Last 34,800 Years from the Southeastern Brazilian Upper Slope: Links between Sea Surface Temperature, Displacement of the Brazil Current, and Marine Productivity. *Geo-Mar Lett.* 36 (5), 361–369. doi:10.1007/s00367-016-0453-7

Mahiques, M. M., Fukumoto, M. M., Silveira, I. C. A., Figueira, R. C. L., Bícego, M. C., Lourenço, R. A., et al. (2007). Sedimentary Changes on the Southeastern Brazilian Upper Slope during the Last 35,000 Years. *An. Acad. Bras. Ciênc.* 79, 171–181. doi:10.1590/S0001-37652007000100018

Michaelovitch de Mahiques, M., Almeida da Silveira, I. C., de Mello e Sousa, S. H., and Rodrigues, M. (2002). Post-LGM Sedimentation on the Outer Shelf-Upper Slope of the Northernmost Part of the São Paulo Bight, Southeastern Brazil. *Mar. Geol.* 181 (4), 387–400. doi:10.1016/S0025-3227(01)00225-0

Molfino, B., and McIntyre, A. (1990). Precessional Forcing of Nutricline Dynamics in the Equatorial Atlantic. *Science* 249 (4970), 766–769. doi:10.1126/science.249.4970.766

Nagai, R. H., Ferreira, P. A. L., Mulkherjee, S., Martins, M. V., Figueira, R. C. L., Sousa, S. H. M., et al. (2014). Hydrodynamic Controls on the Distribution of Surface Sediments from the Southeast South American Continental Shelf between 23°S and 38°S. *Cont. shelf Res.* 89, 51–60. doi:10.1016/j.csr.2013.09.016

Nagai, R. H., Sousa, S. H. D. M., Lourenço, R. A., Bícego, M. C., and Mahiques, M. M. D. (2010). Paleoproductivity Changes during the Late Quaternary in the Southeastern Brazilian Upper Continental Margin of the Southwestern Atlantic. *Braz. J. Oceanogr.* 58, 31–41. doi:10.1590/S1679-87592010000500004

Okada, H., and Honjo, S. (1975). Distribution of Coccolithophores in Marginal Seas along the Western Pacific Ocean and in the Red Sea. *Mar. Biol.* 31 (3), 271–285. doi:10.1007/BF00387154

Okada, H., and Honjo, S. (1973). The Distribution of Oceanic Coccolithophorids in the Pacific. *Deep Sea Res. Oceanogr. Abstr.* 20 (4), 355–374. doi:10.1016/0011-7471(73)90059-4

Okada, H., and McIntyre, A. (1979). Seasonal Distribution of Modern Coccolithophores in the Western North Atlantic Ocean. *Mar. Biol.* 54 (4), 319–328. doi:10.1007/BF00395438

Pedrão, G. A., Costa, K. B., Toledo, F. A. L., Tomazella, M. O., and Jovane, L. (2021). Semi-Quantitative Analysis of Major Elements and Minerals: Clues from a Late Pleistocene Core from Campos Basin. *Appl. Sci.* 11 (13), 6206. doi:10.3390/app11136206

Pereira Brandini, F., Nogueira, M., Jr, Simião, M., Carlos Ugaz Codina, J., and Almeida Noernberg, M. (2014). Deep Chlorophyll Maximum and Plankton Community Response to Oceanic Bottom Intrusions on the Continental Shelf in the South Brazilian Bight. *Cont. Shelf Res.* 89, 61–75. doi:10.1016/j.csr.2013.08.002

Pereira, L. S., Arz, H. W., Pätzold, J., and Portilho-Ramos, R. C. (2018). Productivity Evolution in the South Brazilian Bight during the Last 40,000 Years. *Paleoceanogr. Paleoclimatology* 33 (12), 1339–1356. doi:10.1029/2018PA003406

Piola, A. R., Matano, R. P., Palma, E. D., Möller, O. O., Jr, and Campos, E. J. (2005). The Influence of the Plata River Discharge on the Western South Atlantic Shelf. *Geophys. Res. Lett.* 32, 1. doi:10.1029/2004GL021638

Pivel, M. A. G., Santarosa, A. C. A., Bariani, L., Costa, K. B., and Toledo, F. A. L. (2011). Paleoprodutividade na Bacia de Santos nos últimos 15 mil anos. *Paleontol. Cenários Vida* 3, 333

Portilho-Ramos, R. D. C., Pinho, T. M. L., Chiessi, C. M., and Barbosa, C. F. (2019). Understanding the Mechanisms behind High Glacial Productivity in the Southern Brazilian Margin. *Clim. Past.* 15 (3), 943–955. doi:10.5194/cp-15-943-2019

Razik, S., Govin, A., Chiessi, C. M., and von Dobeneck, T. (2015). Depositional Provinces, Dispersal, and Origin of Terrigenous Sediments along the SE South American Continental Margin. *Mar. Geol.*, 363, 261–272. doi:10.1016/j.margeo.2015.03.001

Reimer, P. J., Bard, E., Bayliss, A., Beck, J. W., Blackwell, P. G., Ramsey, C. B., et al. (2013). IntCal13 and Marine13 Radiocarbon Age Calibration Curves 0-50,000 Years Cal BP. *Radiocarbon* 55 (4), 1869–1887. doi:10.2458/azu_js_rc.55.16947

Roth, P. H. (1994). "Distribution of Coccoliths in Oceanic Sediments," in *Coccolithophores*. Editors A. Winter and W. G. Siesser (Cambridge, U.K): Cambridge University Press), 178

Rühlemann, C., Mulitza, S., Müller, P. J., Wefer, G., and Zahn, R. (1999). Warming of the Tropical Atlantic Ocean and Slowdown of Thermohaline Circulation during the Last Deglaciation. *Nature* 402 (6761), 511–514. doi:10.1038/990069

Saavedra-Pellitero, M., Flores, J. A., Lamy, F., Sierro, F. J., and Cortina, A. (2011). Coccolithophore Estimates of Paleotemperature and Paleoproductivity Changes in the Southeast Pacific over the Past ~27 Kyr. *Paleoceanography* 26, 1. doi:10.1029/2009PA001824

Schneider, T., Bischoff, T., and Haug, G. H. (2014). Migrations and Dynamics of the Intertropical Convergence Zone. *Nature* 513 (7516), 45–53. doi:10.1038/nature13636

Silveira, I. C. A. d., Schmidt, A. C. K., Campos, E. J. D., Godoi, S. S. d., and Ikeda, Y. (2000). A corrente Do Brasil ao largo da costa leste brasileira. *Rev. Bras. Oceanogr.* 48 (2), 171–183. doi:10.1590/S1413-77392000000200008

Spratt, R. M., and Lisiecki, L. E. (2016). A Late Pleistocene Sea Level Stack. *Clim. Past.* 12 (4), 1079–1092. doi:10.5194/cp-12-1079-2016

Stoll, H. M., and Ziveri, P. (2002). Separation of Monospecific and Restricted Coccolith Assemblages from Sediments Using Differential Settling Velocity. *Mar. Micropaleontol.* 46 (1-2), 209–221. doi:10.1016/S0377-8398(02)00040-3

Stramma, L., and England, M. (1999). On the Water Masses and Mean Circulation of the South Atlantic Ocean. *J. Geophys. Res.* 104 (C9), 20863–20883. doi:10.1029/1999JC900139

Sylvestre, F. (2009). "Moisture Pattern during the Last Glacial Maximum in South America," in *Past Climate Variability in South America and Surrounding Regions*. Editors F. Vimeux, F. Sylvestre, and M. Khodri (Dordrecht): Springer), 3–27. doi:10.1007/978-90-481-2672-9_1

Toledo, F. A. L., Cachão, M., Costa, K. B., and Pivel, M. A. G. (2007). Planktonic Foraminifera, Calcareous Nannoplankton and Ascidian Variations during the Last 25 Kyr in the Southwestern Atlantic: A Paleoproductivity Signature? *Mar. Micropaleontol.* 64 (1-2), 67–79. doi:10.1016/j.marmicro.2007.03.001

Toledo, F. A. L., Quadros, J. P., Camillo, E., Jr, Santarosa, A. C. A., Flores, J.-A., and Costa, K. B. (2016). Plankton Biochronology for the Last 772,000 Years from the Western South Atlantic Ocean. *Mar. Micropaleontol.* 127, 50–62. doi:10.1016/j.marmicro.2016.07.002

Toledo, F. A. L. (2000). "*Variações Paleoceanográficas nos últimos 30.000 anos no oeste Do Atlântico Sul: Isótopos de oxigênio, assembléias de foraminíferos planctônicos e nanofósseis calcários*," (Brazil: [Geoscience Institute]: Federal Univ. Rio Grande do Sul). PhD Thesis.

Toledo, F., Costa, K. B., Pivel, M. A., and Campos, E. J. (2008). Tracing Past Circulation Changes in the Western South Atlantic Based on Planktonic Foraminifera. *Rev. Bras. Paleontol.* 11 (3), 169–178. doi:10.4072/rbp.2008.3.03

Tyrrell, T., and Merico, A. (2004). "*Emiliania Huxleyi*: Bloom Observations and the Conditions that Induce Them," in *Coccolithophores* (Berlin, Heidelberg: Springer), 75–97. doi:10.1007/978-3-662-06278-4_4

Vera, C., Silvestri, G., Liebmann, B., and González, P. (2006). Climate Change Scenarios for Seasonal Precipitation in South America from IPCC-AR4 Models. *Geophys. Res. Lett.* 33 (13), 13707–13711. doi:10.1029/2006GL025759

Viana, A. R., Faugères, J. C., Kowsmann, R. O., Lima, J. A. M., Caddah, L. F. G., and Rizzo, J. G. (1998). Hydrology, Morphology and Sedimentology of the Campos Continental Margin, Offshore Brazil. *Sediment. Geol.* 115 (1-4), 133–157. doi:10.1016/S0037-0738(97)00090-0

Vidal, L., Schneider, R. R., Marchal, O., Bickert, T., Stocker, T. F., and Wefer, G. (1999). Link between the North and South Atlantic during the Heinrich Events of the Last Glacial Period. *Clim. Dyn.* 15 (12), 909–919. doi:10.1007/s003820050321

Wang, X., Auler, A. S., Edwards, R. L., Cheng, H., Ito, E., Wang, Y., et al. (2007). Millennial-scale Precipitation Changes in Southern Brazil over the Past 90,000 Years. *Geophys. Res. Lett.* 34 (23), n/a–n/a. doi:10.1029/2007gl031149

Weltje, G. J., and Tjallingii, R. (2008). Calibration of XRF Core Scanners for Quantitative Geochemical Logging of Sediment Cores: Theory and Application. *Earth Planet. Sci. Lett.* 274, 423–438. doi:10.1016/j.epsl.2008.07.054

Winter, A., Jordan, R. W., and Roth, P. H. (1994). "Biogeography of Living Coccolithophores in Ocean Waters," in *Coccolithophores*. Editors A. Winter and W. G. Siesser (CambridgeCambridge, U.K): Cambridge University Press), 161

Young, J. R. (1994). "Functions of Coccoliths," in *Coccolithophores*. Editors A. Winter and W. G. Siesser (Cambridge, U.K: Cambridge University Press), 63

Zhou, X., Duchamp-Alphonse, S., Kageyama, M., Bassinot, F., Beaufort, L., and Colin, C. (2020). Dynamics of Primary Productivity in the Northeastern Bay of Bengal over the Last 26 000 Years. *Clim. Past.* 16 (5), 1969–1986. doi:10.5194/cp-16-1969-2020

Conflict of Interest: The authors declare that the research was conducted in the absence of any commercial or financial relationships that could be construed as a potential conflict of interest.